Quantum charging advantage based on power bounds can be deceptive

Sreeram PG,[1,*] J. Bharathi Kannan,[1,†] and M. S. Santhanam[1,‡]

[1] *Department of Physics, Indian Institute of Science Education and Research, Pune 411008, India*

We demonstrate that an all-to-all coupled spin-chain model of a quantum battery with 2-local interactions exhibits superextensive charging when analysed using the upper bound derived from the uncertainty principle. Unlike the previously studied models in the literature, the contribution to this apparent quantum advantage arises from both the battery and the charger, and it does not require long-range couplings. However, on closer analysis of the charging using the battery evolution in the energy eigenspace, the advantage vanishes. Moreover, this tighter bound can also fail in certain physical situations. One has to exercise caution and compute the actual power transferred before claiming a quantum advantage.

I. INTRODUCTION

Rapid advancements in the field of quantum information have sparked interest in using quantum effects to enhance the performance of technologies other than quantum computation. Energy storage using quantum batteries is one such area which has shown considerable theoretical progress [1, 2].

A quantum battery is a quantum system that can be manipulated through unitary operations to store and release energy [1–8]. The maximum amount of energy one can unitarily extract or deposit in a quantum battery is called the *ergotropy* [3, 9–13]. In a seminal work, Alicki and Fannes demonstrated quantum advantage in ergotropy in the presence of quantum correlations [3]. However, subsequent research found that the advantage is only in the number of operations required to charge the battery [14], and not in the magnitude of the energy stored or extracted. This shifted the focus to the charging power [2], i.e., the energy deposited per unit time. For a quantum battery described by the state ρ, and the governing Hamiltonian being H_B, the charging power is defined as

$$P(t) = \mathrm{Tr}[(\rho' - \rho)H_B]/t, \tag{1}$$

where ρ' is the time evolved state and t is the charging time. A quantum battery consisting of N cells (spins) can charge N times faster if the cells are globally coupled, compared to charging them independently [15]. As the former is achieved due to quantum correlations among the N cells, the latter scenario of independent charging without the aid of these correlations is usually referred to as "classical". Though quantum correlations among the cells help achieve speedup, in practice, collective charging with complex global correlations is necessary for a potentially extensive ($\sim N$) advantage [16].

The instantaneous charging power is upper bounded in terms of the battery Hamiltonian H_B, and the charging Hamiltonian $H_C(t)$. The upper bound can be obtained from the Robertson uncertainty relation as [17],

$$P(t)^2 \leq 4\ \Delta H_B(t)^2\ \Delta H_C(t)^2, \tag{2}$$

where ΔH^2 represents the variance of Hamiltonian H. To avoid spurious charging from non-quantum effects, H_C must be well defined in the thermodynamic limit of large N. Superextensive scaling of H_C can lead to fictitious quantum advantage observed in Ref. [4, 18] and pointed out in Ref. [19].

How does the power bound capture a potential quantum advantage? Simulation results indicate that larger entanglement typically leads to enhanced non-local charging process, resulting in quantum advantage. The charger Hamiltonian H_C is the resource that drives the charging process by delocalizing the battery state and inducing pronounced overlaps with higher energy eigenstates of H_B. In this sense, ΔH_B^2 is an indirect indicator of the amount of entanglement between the cells in the battery, and ΔH_C^2 sets a bound on how fast energy can be transferred into the battery per unit time.

Proper scaling of the energy resource H_C is crucial, as undue advantage can arise even when H_C is extensive. For example, the unnatural scaling of H_C by the particle number N for a *fair* comparison with the parallel charging [15, 20] results in inflated quantum charging. Here, the scaling by N is imposed so that the available energy for quantum charging scales the same way as in the classical case. While H_C remains extensive in this case, the scaling factor increases the coupling strength between cells, leading to inflated charging [17]. Julià-Farré et al. [17] found that under a fair physical constraint – specifically, a limit on the maximum available energy or strength of the charging field – quantum advantage does not manifest as a superlinear scaling of power with $P \sim N^\alpha$ with $\alpha > 1$, but rather as a dramatic reduction in the resources required to achieve the classical scaling of power ($P \sim N$). They proposed a more physically meaningful and tighter bound to charging power by replacing $\Delta H_C(t)^2$ by Fisher information $I_E(t)$ [17]:

$$P(t)^2 \leq\ \Delta H_B(t)^2\ I_E(t). \tag{3}$$

Fisher information captures the "speed" of the battery state evolution in the energy eigenspace, by quantifying

* sreerampg7@gmail.com
† bharathikannan1130@gmail.com
‡ santh@iiserpune.ac.in

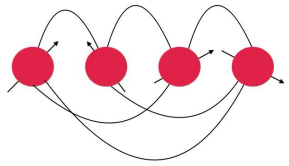

FIG. 1: A schematic of an all-to-all interacting spin chain model with 2-local interactions. The chain shows only $N = 4$ spins for clarity.

the probability current. For a mathematical definition of $I_E(t)$, look at Eq. 9. For the same amount of probability current flow ($I_E(t)$), a system with more entanglement, and consequently a larger ΔH_B^2, can leverage more charging power as Eq. 3 suggests. While the charger H_C is the driving force behind the battery system traversing the energy space, a larger $\Delta H_B^2\ \Delta H_C^2$ in collective charging only indicates the potential for a quantum advantage. A larger bound than parallel charging does not guarantee a tangible quantum enhancement. On the other hand, I_E captures the actual *activity* in the battery energy space by quantifying the rate of change of energy distribution of the battery. Importantly, this also makes the power bound independent of H_C. However, I_E may also lead to loose bounds in charging, as all the activity in energy space may not strictly correspond to charging. It might also indicate discharging process.

To probe these interconnected issues related to quantum advantage in batteries, in this article, we study an all-to-all coupled spin-chain quantum battery with 2-local interactions (two-body interactions). We find that computing the bound $\Delta H_B^2\ \Delta H_C^2$ suggests that the system can exhibit a near-optimal quantum charging advantage despite the lack of global interactions. However, upon further scrutiny, we find that the battery state's evolution in the energy basis does not show faster charging with increasing N. This prompts us to study the power bounds more closely. While these bounds are well-founded physically and can even be reached in certain cases, they also may not accurately represent the underlying energy dynamics in specific situations. The findings from this work do not challenge the power bounds themselves. They are theoretically elegant and insightful about the mechanism of the quantum advantage, and should be studied. However, in an eagerness to claim quantum supremacy, one should not overlook a more detailed analysis, as the upper bounds as a standalone measure can be quite loose for the system at hand.

In the next section, we introduce a kicked spin chain model of a quantum battery, and show that the power bound can nearly saturate the quadratic scaling even without global coupling. In Section III, we conduct a closer inspection of the charging using the battery evolution in the energy eigenspace, and show that the advantage vanishes. We resolve the apparent contradiction between the two treatments and remark on using power bounds as a standalone measure of quantum advantage in Section IV.

II. KICKED SPIN CHAIN MODEL OF QUANTUM BATTERY AND SUPEREXTENSIVE POWER BOUND

The model of spin-chain quantum battery consists of two parts; a battery Hamiltonian given by

$$H_B = J_z = \sum_{i=1}^{N} \sigma_z^i, \tag{4}$$

and a charger Hamiltonian H_c represented by a collection of spins to which instantaneous kicks of strength β are imparted at periodic intervals of τ [21–23]:

$$H_C = \frac{\pi}{2} J_y + \beta \frac{J_z^2}{2j} \sum_n \delta(t - n\tau). \tag{5}$$

In this, the angular momentum operators are composed of smaller spins [24–26], i.e., $J_\alpha = \sum_{i=1}^{N} \sigma_\alpha^i$, where $\alpha = x, y, z$ with N being the number of spins in the chain, and σ_α are the Pauli matrices for spin-$\frac{1}{2}$. In terms of individual spins, the Hamiltonian H_C can be explicitly written as

$$H_C = \frac{\pi}{2} \sum_{i=1}^{N} \sigma_y^i + \beta \frac{\left(\sum_{i=1}^{N} \sigma_z^i\right)^2}{2j} \sum_n \delta(t - n\tau). \tag{6}$$

In H_C, the term $J_z = \left(\sum_{i=1}^{N} \sigma_z^i\right)^2$ leads to coupling of each spin with every other spin via two-body interactions as shown in Fig. 1. During the time interval between consecutive kicks, only $J_y = \sum_{i=1}^{N} \sigma_y^i$ term is present, leading to a continuous precession. At the instance of a kick, the impulsive nonlinear torsion is turns on, whose strength is determined by β. Physically, such delta kicks are realized by brief electromagnetic pulses—either at radio frequencies or in the microwave range—or via direct magnetic field pulses, depending on the experimental platform [22, 23, 27]. The kicks could be modelled by a strong square pulse lasting $\epsilon \to 0$ in time, with the strength $f(t) \sim 1/\epsilon$, acting periodically. Therefore, at the kicks, the physical Hamiltonian becomes $H_C = \frac{\pi}{2} J_y + \beta \frac{J_z^2}{2j} \times f(t)$, Since $f(t)$ does not vary with system size, we may as well set $f(t) = 1$ to check the extensivity of the Hamiltonian.

Figure 2 displays the norm and variance of H_C. At instants when kicks are applied, $H_C = \frac{\pi}{2} J_y + \beta \frac{J_z^2}{2j}$ with $\beta = 7$, and during the time interval between consecutive kicks $H_C = \frac{\pi}{2} J_y$. Note that $\beta = 7$ is the fully chaotic regime for H_C. It is clear from Fig. 2(a) that the kicked spin chain Hamiltonian H_C is extensive at the instants of kicks and in between kicks. As the numerical results show in Fig. 2(a), J_y and $J_z^2/2j$ scale linearly with N,

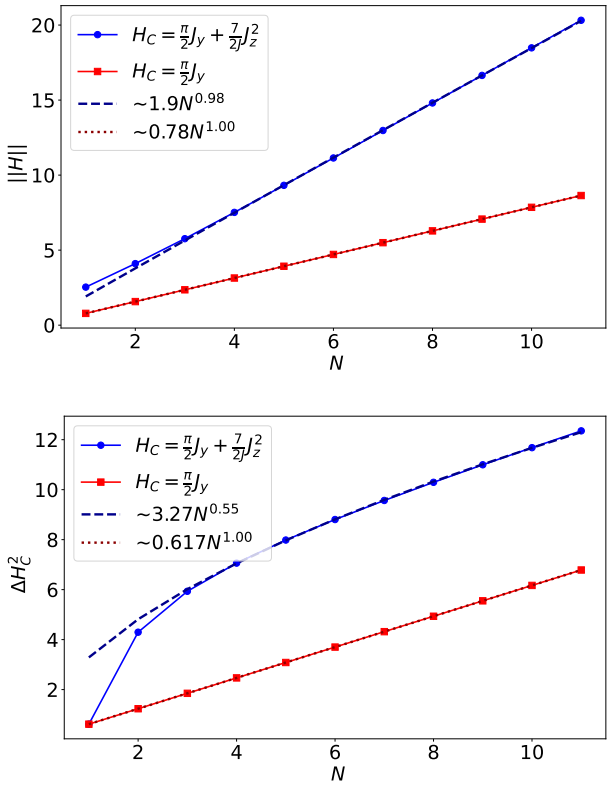

FIG. 2: (a) Mean eigenvalue and (b) variance of the eigenvalues of H_C at the kicks ($H_C = \frac{\pi}{2}J_y + \frac{7}{2j}J_z^2$) and in between the kicks ($H_C = \frac{\pi}{2}J_y$).

and therefore the mean energy growing linearly ($\sim N$) is to be expected.

The variance of H_C is shown in Fig. 2(b). The eigenvalue variance (between successive kicks) of $\frac{\pi}{2}J_y$ scales linearly because of its composite structure being a sum of Pauli matrices and the resulting degeneracies. For any given projection quantum number m, there are $\binom{N}{j+m}$ possible configurations where $m \in \{-j, -j+1, \ldots, j-1, j\}$. This is unlike the case of single particle ($N = 1$), in which J_y operator will have no degeneracies, and its variance would scale quadratically. Now assume that $\beta \gg 0$ where the kicking term dominates, so that the Hamiltonian effectively reduces to $H_C \approx \frac{J_z^2}{2j}$ at the instants of kicks. The energy eigenvalue of $\frac{J_z^2}{2j}$ is of the form $E = \frac{m^2}{2j}$. The J_z operator, with a composite structure as a sum of N Pauli operators, also has the same degeneracies as J_y just discussed. As a result, under this circumstance, the variance ΔJ_z^2 only scales quadratically ($\sim N^2$), whereas in the corresponding single particle case ΔJ_z^2 scales as $\sim N^4$. Furthermore, the $1/j^2$ factor makes the $\left(\Delta \frac{J_z^2}{2j}\right)^2 = \frac{1}{4j^2}\left(\langle J_z^4\rangle - \langle J_z^2\rangle^2\right)$ independent of N. The arguments in this and the previous paragraphs, when taken together, explain the sublinear scaling of the ΔH_C^2 at the instants of kicks for $\beta = 7$, where both J_y and J_Z^2 terms contribute (Fig. 2(b)).

Notice that we have taken static Hamiltonians at the instant of kicks and in between the kicks, each of which is separately an integrable system. This is used for verifying thermodynamic consistency, i.e., ruling out superextensive energy growth at all times. The full Hamiltonian in Eq. 6 is time-dependent and chaotic due to the non-commutativity between the term that generates constant precession ($\sum_{i=1}^N \sigma_y^i$), and the one generating periodic torsion $\left(\sum_{i=1}^N \sigma_z^i\right)^2$. We note that extensivity and integrability are independent properties. We separate the time-dependent, chaotic Hamiltonian into static integrable ones only for the purpose of understanding the scaling with respect to N.

Having characterised the charger, for further analysis, the internal battery is chosen to be the Hamiltonian in Eq. 4. It must be noncommuting with H_C and have an additive structure, so that the battery is composed of N independent cells. Since the charger is a periodically kicked system of Eq. 5, time evolution reduces to stroboscopic tracking of the dynamics. The evolution of the battery state over one time step is obtained from Eq. 6 as

$$U_C(\tau) = \exp\left(-\frac{\pi}{2}\sum_{i=1}^N \sigma_y^i\right)\exp\left(\frac{\beta}{2j}\left(\sum_{i=1}^N \sigma_z^i\right)^2\right). \quad (7)$$

The battery charging time is fixed to be 50 time steps, i.e., 50 applications of $U_C(\tau)$), for analysis. We choose the initial state to be the fully discharged state of the battery Hamiltonian, given by the coherent initial state, with ($\theta = \pi, \phi = 0$), denoted by $|\theta, \phi\rangle$ [21]:

$$|\theta, \phi\rangle = \exp\{i\theta(J_x \sin(\phi) - J_y \cos(\phi))\}\,|j, j\rangle\,, \quad (8)$$

where $|j, j\rangle$ denotes a simultaneous eigenvector of J^2 and J_z, with all the spins pointing up.

Probing the average power bound scaling over the course of charging as a function of the particle number N, it is found that $P = 2\Delta J_z \Delta H_C = 0.59N^{1.9}$ (shown in Fig. 3), close to quadratic scaling! The variances of battery and charger are shown as a function of N in the inset of this figure. The maximum bound on power, achievable with a globally interacting charger of the form $H_C^{\#} = \lambda \bigotimes_{i=1}^N h_C^i$, where h_C^i is a local operator on the i^{th} spin, is quadratic in N. A global operation of the form $H_C^{\#}$ leads to genuine multipartite entanglement among the cells, resulting in the quadratic scaling.

However, H_C in Eq. 6 only has two-body interactions, although every spin (cell) is coupled to every other. GHZ-like states with genuine multipartite entanglement are possible in this model, but only if β obeys the resonance condition of $\beta = 4\pi jr/s$, where r and s are co-prime integers [28]. The charger H_C cannot operate at resonance, as the static Hamiltonian becomes superextensive. However, even for the choice of $\beta = 7$ and the fully

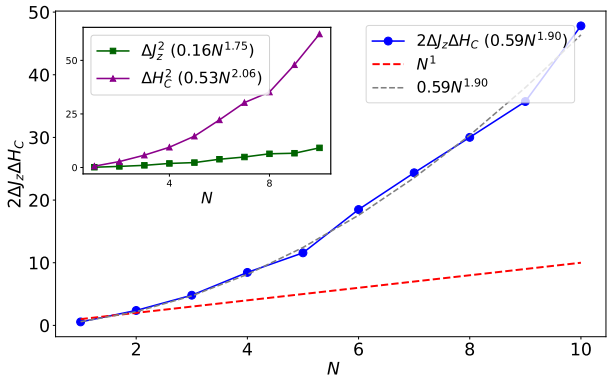

FIG. 3: Power scaling in the spin chain battery with the periodically kicked charging, averaged over 50 time steps is close to quadratic ($\sim N^{1.9}$). The N^1 line shows the classical scaling. The inset shows the individual scalings of the battery and the charger variances.

discharged initial state ($\theta = \pi$, $\phi = 0$), there is a good amount of entanglement generated by the dynamics. The time-averaged variance of the battery Hamiltonian over 50 time-steps scales as $\Delta J_z^2 \sim N^{1.78}$, and $\Delta H_C^2 \sim N^{2.06}$. The exponent values were extimated through a numerical regression. The charger variance ΔH_C^2, computed with respect to the evolved states, is superextensive despite the static Hamiltonian scaling subextensively at the kicks and extensively in between successive kicks (Fig. 2). An initial state evolves into highly nonclassical states involving significant quantum correlations, and the variance grows superlinearly, even though the bare Hamiltonian satisfies the thermodynamic consistency condition. In the charger, as β increases, ΔH_C^2 grows increasingly superlinear, indicating the quantum origin of such superextensivity. This, combined with the superextensive variance of H_B is the origin of the quantum advantage.

The above analysis suggests that we can potentially achieve a quadratic scaling without global interactions! Moreover, the 2-local coupling discussed in this model is also experimentally friendly compared to the fragile global interactions. Together, this sounds sensational, but we need further analysis to verify. In the next section, a series of different scenarios are considered to understand the import of the power bounds.

III. ENERGY SPACE ACTIVITY AND THE VANISHING POWER ADVANTAGE

Instead of using ΔH_C^2 in the upper bound as in Eq. 2, using the evolution speed in energy eigenspace of the battery as quantified by Fisher information results in a tighter upper bound, as $I_E \leq 4\Delta H_C^2$ [17]. To define Fisher Information I_E, consider the battery Hamiltonian in the diagonal form; $H_B = \sum E_k P_k$, where E_k are the energy eigenvalues, and P_k the corresponding eigenvector projectors. For the battery state $\rho(t)$ with projection $p_k(t) = \mathrm{Tr}(P_k \rho(t))$ with the k^{th} eigenvector, I_E is defined as [17]:

$$I_E(t) = \sum_k \left(\frac{d}{dt} \log_2(p_k(t)) \right)^2 p_k(t), \tag{9}$$

$$\approx \frac{2D_{\mathrm{KL}}(\bar{p}(t+\delta t)||\bar{p}(t))}{\delta t^2}. \tag{10}$$

Here $D_{\mathrm{KL}}(.||.)$ denotes the Kullback-Leibler (KL) divergence [29] between two probability distributions incrementally apart in time. The KL divergence between two probability distributions $\bar{p}$ and $\bar{q}$ is defined as

$$D_{\mathrm{KL}}(\bar{p}||\bar{q}) = \sum_k p_k \log_2 \frac{p_k}{q_k}. \tag{11}$$

In the absence of continuous derivatives, we compute the KL divergence between the probabilities after each time step (kick), consistent with the physical intuition provided by Eq. 9. However, upon increasing the particle number N, it is observed that the energy space activity captured by the time-averaged $D_{\mathrm{KL}}(\bar{p}(n+1)||\bar{p}(n))$ does not scale with N, and remains almost identical, as shown in Fig. 4. What does a nearly constant KL divergence imply about charging despite the superlinear scaling of ΔH_B^2 and ΔH_C^2? This indicates that despite the rapid spreading of the state in the Hilbert space, the probability flow between different energy levels is surprisingly slow. The scrambling in the Hilbert space is due to the chaotic charging operator. However, rapid spreading in the Hilbert space is not the same as evolution in the energy eigenspace. Two orthogonal states in the Hilbert space can have identical energy distribution. The chaotic H_C can scramble the state in the Hilbert space, but does not lead to an effectively directed energy flow.

Under the improved power bound in Eq. 3 [17], both the quantum and parallel charging protocols achieve the same power. The parallel protocol achieves average power $P \sim N$ through a large Fisher information, $I_E \sim N$, generated by its N independent components, but with a limited variance $\Delta H_B^2 \sim N$ from its product state. The global protocol on the other hand achieves the same $P \sim N$ through a large variance, $\Delta H_B^2 \sim N^2$, from its entangled state, which compensates for a small Fisher information ($I_E \sim$ constant) from its single pulse.

But the quantum advantage has not vanished under the improved bound. Now the advantage resides in the resources required to charge the battery at the same power as in the classical case. The energy scales as $||H_C^{\#}|| \sim \lambda$ for a global charger of the form $H_C^{\#} = \lambda \bigotimes_{i=1}^{N} h_C^i$. This energy does not change with N. The hardware complexity is also low, as a single global control device (e.g., lasers, microwave pulse, etc.) is sufficient for charging. In parallel charging scenario, $H_C^{||} = \sum_{i=1}^{N} \lambda h_C^i$, the hardware complexity and the energy $||H_C^{||}||$ scale extensively $\sim N$, as independent chargers must be powered for each cell.

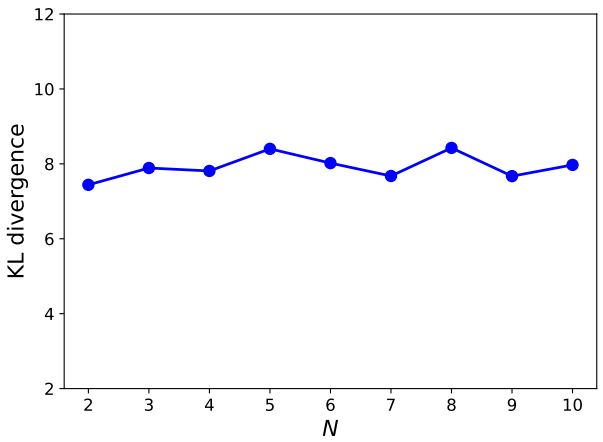

FIG. 4: KL divergence averaged over 50 time steps, as a function of the number of spins.

IV. DOES MORE ENERGY SPACE ACTIVITY ALWAYS MEAN BETTER CHARGING?

Does a significant energy space activity, given by $D_{\mathrm{KL}}(\bar{p}(n+1)||\bar{p}(n))$, always mean better power? Not all probability changes result in a strict increase in the battery's energy storage, as shown below. The following situations arise because the differential form of the energy space activity defined by I_E in the improved bound is blind to the energy scale of the problem.

A. I_E does not recognize the magnitude of energy transfer

Consider a battery system-1 with two non-degenerate but very close energy levels with battery Hamiltonian: $H_B^1 = \begin{pmatrix} 0 & 0 \\ 0 & \epsilon \end{pmatrix}$ with ϵ very small, and a battery-2 where $H_B^2 = \begin{pmatrix} 0 & 0 \\ 0 & 1 \end{pmatrix}$. The battery Hamiltonians differ only in their energy gap. We take the initial state in both systems to be $|1\rangle$ and charge them with the Hamiltonian: $H_C = \lambda\sigma_x$. The time evolution operator for both systems is given by

$$U(t) = e^{-iH_C t} = \cos(\lambda t)I - i\sin(\lambda t)\sigma_x. \tag{12}$$

The state at time t is:

$$|\psi(t)\rangle = U(t)\,|\psi_0\rangle = \cos(\lambda t)\,|1\rangle - i\sin(\lambda t)\,|0\rangle\,. \tag{13}$$

The population in each eigenstate is the same in both batteries and is given by $p_1(t) = \cos^2(\lambda t)$, and $p_0(t) = \sin^2(\lambda t)$. Then, expanding Eq. 9,

$$I_E(t) = \frac{\dot{p}_0^2}{p_0} + \frac{\dot{p}_1^2}{p_1} = \lambda^2\frac{\sin^2(2\lambda t)}{\sin^2(\lambda t)} + \lambda^2\frac{\sin^2(2\lambda t)}{\cos^2(\lambda t)}. \tag{14}$$

I_E is the same regardless of the energy scale. The energy transfer is minimal, $P(t) \sim \epsilon$, in battery-1 because ϵ is small. However, I_E can be large because the populations are changing rapidly. On the other hand, $P(t) \sim 1$ in battery-2, and I_E at any given time is the same as that of battery-1.

B. I_E does not recognize wasteful discharge of the battery

Since I_E only captures the change in the energy space distribution, it is blind to the direction of the energy flow. Using the form in Eq. 14, $I_E(t)$ is defined as

$$I_E(t) = \sum_k \frac{\dot{p}_k^2}{p_k}. \tag{15}$$

Notice that only squares of the time derivatives of p_k appear in the above definition. Therefore, I_E is invariant with respect to the time reversal transformation, which results in $\dot{p}_k \to -\dot{p}_k$. Hence, I_E fails to recognize charging from discharging.

For example, consider a simple qubit battery ($H_B = \frac{1}{2}\sigma_z$) undergoing Rabi oscillations driven by $H_C = \lambda\sigma_x$. Assume that the system starts in the fully discharged state $|\psi_0\rangle = |1\rangle$, as in the previous example. From Eq. 13, one can see that the battery is fully charged (reaching $|0\rangle$) at $t = \pi/2\lambda$. beyond this time, the battery is in the discharging phase until $t = \pi/\lambda$, where $P(t) < 0$. The functional expression for $I_E(t)$ is the same as the previous case, and is given by Eq. 14. One can verify from Eq. 14 that

$$I_E(t) = I_E\left(\frac{\pi}{\lambda} - t\right), \tag{16}$$

where $0 \le t \le \pi/2\lambda$. Thus, at time t (charging) and time $(\pi/\lambda - t)$ (discharging), the Fisher Information I_E is identical, but the power $P(t)$ has the same magnitude and opposite sign.

This example indicates that the upper bound containing I_E can be misleading if used in isolation. A high I_E can indicate efficient charging or rapid, wasteful self-discharge. One cannot distinguish a healthy battery from a faulty one using I_E alone.

C. I_E can be large due to dynamics within a degenerate subspace.

Consider a battery Hamiltonian with a degenerate subspace:

$$H_B = \begin{pmatrix} 0 & 0 & 0 \\ 0 & 0 & 0 \\ 0 & 0 & 1 \end{pmatrix} \tag{17}$$

H_B has two degenerate ground state levels $\{|g_1\rangle\,\&\,|g_2\rangle\}$ with energy $E = 0$, and an excited level $|e\rangle$ at $E = 1$.

Now, consider a charging Hamiltonian that only couples the two degenerate levels: $H_C = \lambda(|g_1\rangle\langle g_2| + |g_2\rangle\langle g_1|)$. For an initial state $|\psi_0\rangle = |g_1\rangle$, whose dynamics according to H_C is completely confined to the degenerate subspace, the Hamiltonian can be represented as a 2×2 matrix in the $\{|g_1\rangle, |g_2\rangle\}$ basis:

$$H_C = \lambda \begin{pmatrix} 0 & 1 \\ 1 & 0 \end{pmatrix}. \tag{18}$$

Then the evolved state is given by $|\psi(t)\rangle = \cos(\lambda t)|g_1\rangle - i\sin(\lambda t)|g_2\rangle$. Again, in this case, $I_E(t)$ is the same as Eq. 14:

$$I_E(t) = \frac{\dot{p}_{g_1}^2}{p_{g_1}} + \frac{\dot{p}_{g_2}^2}{p_{g_2}} = \lambda^2 \frac{\sin^2(2\lambda t)}{\sin^2(\lambda t)} + \lambda^2 \frac{\sin^2(2\lambda t)}{\cos^2(\lambda t)}. \tag{19}$$

Equation 19 is in general nonzero, even though the battery state is only hopping between two degenerate levels. There is no charging taking place in this case, and both the $\langle H_B\rangle_{\psi(t)}$ and $P(t) = 0\ \forall t$. However, $I_E(t)$ fails to recognize this, which is a critical flaw. The activity measured by I_E is entirely wasted on population changes within a degenerate energy level, resulting in no net energy transfer to the battery.

D. I_E can diverge at a turning point where $P(t) = 0$.

The Fisher Information can diverge even when the power is zero, typically at points where the population of an energy level approaches zero. In the Rabi oscillation example of Sec IVB, consider $t = \pi/2\lambda$, where $p_0 = 1$ and $p_1 = 0$. The battery is fully charged and the energy is maximum, with $P(t) = \frac{dE}{dt} = 0$. At this instant, there is no charging taking place. However, $I_E(t)$ diverges at this point as $p_0 \to 0$ in Eq. 14. Thus, the Fisher information metric is unstable at the inflection points, where the system changes from charging to discharging or vice versa.

V. DISCUSSION AND CONCLUSION

We studied a kicked spin model of a quantum battery, which exhibits a nearly quadratic power advantage, despite lacking global interactions. However, the advantage disappeared on a closer examination of the state evolution in the energy eigenspace. Although there is a significant entanglement generation in this model, it does not reflect as a resource advantage in the collective charging process. We also demonstrated that the stronger upper bound using Fisher information, which captures energy space activity, may fail in certain specific situations. One has to be careful while claiming a quantum advantage based only on the power bounds, as they may be quite loose for the system at hand.

The variances of H_B and H_C at a given time are relatively easy to measure experimentally compared to Fisher information, particularly when they have simple forms. For example, $H_B = \sum_{i=1}^{N} \sigma_z^i$ used in this paper is the total magnetization, and is experimentally amenable as a collective observable in many settings [30–36]. A charger Hamiltonian H_C, when it involves complex interactions and time dependence, could be more challenging to estimate its variance. On the other hand, though Fisher information is a better theoretical tool, it is also difficult to track experimentally. It requires the knowledge of individual populations p_k for all relevant energy levels k. The number of eigenvector projections scales exponentially with system size. Furthermore, computing I_E at any given instant involves a time derivative, and state characterization at nearby points is also necessary. All this makes I_E difficult for experimental estimation.

A more accurate, experimenally friendly power bound that reflects the actual energy flow, without the problems discussed in the previous section, is an interesting future direction. A complete theory needs to incorporate how the geometry of the battery's energy spectrum (H_B) and the nature of the dynamics (H_C) interact to determine the useful, non-wasteful part of I_E that actually contributes to charging. Such a theory will make the study of quantum enhancement unambiguous for quantum batteries. A pragmatic way to verify quantum advantage claims until then is to explicitly determine $P(t) = \frac{d\langle H_B\rangle}{dt}$ experimentally, along with a proper characterization of the resources required to achieve the same.

VI. ACKNOWLEDGEMENTS

S.PG acknowledges the I-HUB quantum technology foundation (I-HUB QTF) based in IISER Pune for financial support.

[1] Francesco Campaioli, Stefano Gherardini, James Q Quach, Marco Polini, and Gian Marcello Andolina. Colloquium: quantum batteries. Reviews of Modern Physics, 96(3):031001, 2024.

[2] James Q Quach, Giulio Cerullo, and Tersilla Virgili. Quantum batteries: The future of energy storage? Joule, 7(10):2195–2200, 2023.

[3] Robert Alicki and Mark Fannes. Entanglement boost for extractable work from ensembles of quantum batteries. Physical Review E—Statistical, Nonlinear, and Soft Matter Physics, 87(4):042123, 2013.

[4] Thao P Le, Jesper Levinsen, Kavan Modi, Meera M Parish, and Felix A Pollock. Spin-chain model of a many-body quantum battery. Physical Review A, 97(2):022106, 2018.

[5] I Maillette de Buy Wenniger, SE Thomas, M Maffei, SC Wein, M Pont, N Belabas, S Prasad, A Harouri, A Lemaître, I Sagnes, et al. Experimental analysis of energy transfers between a quantum emitter and light fields. Physical Review Letters, 131(26):260401, 2023.

[6] Alan C Santos, Barış Çakmak, Steve Campbell, and Nikolaj T Zinner. Stable adiabatic quantum batteries. Physical Review E, 100(3):032107, 2019.

[7] Fu-Quan Dou, Yuan-Jin Wang, and Jian-An Sun. Highly efficient charging and discharging of three-level quantum batteries through shortcuts to adiabaticity. Frontiers of Physics, 17(3):31503, 2022.

[8] Borhan Ahmadi, Paweł Mazurek, Paweł Horodecki, and Shabir Barzanjeh. Nonreciprocal quantum batteries. Physical Review Letters, 132(21):210402, 2024.

[9] Armen E Allahverdyan, Roger Balian, and Th M Nieuwenhuizen. Maximal work extraction from finite quantum systems. Europhysics Letters, 67(4):565, 2004.

[10] Akira Sone and Sebastian Deffner. Quantum and classical ergotropy from relative entropies. Entropy, 23(9):1107, 2021.

[11] Salvatore Tirone, Raffaele Salvia, and Vittorio Giovannetti. Quantum energy lines and the optimal output ergotropy problem. Physical Review Letters, 127(21):210601, 2021.

[12] Sreeram PG, J Bharathi Kannan, S Harshini Tekur, and MS Santhanam. Dichotomy in the effect of chaos on ergotropy. Physical Review B, 111(5):054314, 2025.

[13] Akram Touil, Barış Çakmak, and Sebastian Deffner. Ergotropy from quantum and classical correlations. Journal of Physics A: Mathematical and Theoretical, 55(2):025301, 2021.

[14] Karen V Hovhannisyan, Martí Perarnau-Llobet, Marcus Huber, and Antonio Acín. Entanglement generation is not necessary for optimal work extraction. Physical review letters, 111(24):240401, 2013.

[15] Felix C Binder, Sai Vinjanampathy, Kavan Modi, and John Goold. Quantacell: powerful charging of quantum batteries. New Journal of Physics, 17(7):075015, 2015.

[16] Ju-Yeon Gyhm, Dominik Šafránek, and Dario Rosa. Quantum charging advantage cannot be extensive without global operations. Physical Review Letters, 128(14):140501, 2022.

[17] Sergi Julià-Farré, Tymoteusz Salamon, Arnau Riera, Manabendra N Bera, and Maciej Lewenstein. Bounds on the capacity and power of quantum batteries. Physical Review Research, 2(2):023113, 2020.

[18] Dario Ferraro, Michele Campisi, Gian Marcello Andolina, Vittorio Pellegrini, and Marco Polini. High-power collective charging of a solid-state quantum battery. Physical review letters, 120(11):117702, 2018.

[19] Davide Rossini, Gian Marcello Andolina, Dario Rosa, Matteo Carrega, and Marco Polini. Quantum advantage in the charging process of sachdev-ye-kitaev batteries. Physical Review Letters, 125(23):236402, 2020.

[20] Francesco Campaioli, Felix A Pollock, Felix C Binder, Lucas Céleri, John Goold, Sai Vinjanampathy, and Kavan Modi. Enhancing the charging power of quantum batteries. Physical review letters, 118(15):150601, 2017.

[21] Fritz Haake, M Kuś, and Rainer Scharf. Classical and quantum chaos for a kicked top. Zeitschrift für Physik B Condensed Matter, 65(3):381–395, 1987.

[22] S Chaudhury, A Smith, BE Anderson, S Ghose, and Poul S Jessen. Quantum signatures of chaos in a kicked top. Nature, 461(7265):768–771, 2009.

[23] VR Krithika, VS Anjusha, Udaysinh T Bhosale, and TS Mahesh. Nmr studies of quantum chaos in a two-qubit kicked top. Physical Review E, 99(3):032219, 2019.

[24] Shohini Ghose, Rene Stock, Poul Jessen, Roshan Lal, and Andrew Silberfarb. Chaos, entanglement, and decoherence in the quantum kicked top. Physical Review A—Atomic, Molecular, and Optical Physics, 78(4):042318, 2008.

[25] Shruti Dogra, Vaibhav Madhok, and Arul Lakshminarayan. Quantum signatures of chaos, thermalization, and tunneling in the exactly solvable few-body kicked top. Physical Review E, 99(6):062217, 2019.

[26] PG Sreeram, Vaibhav Madhok, and Arul Lakshminarayan. Out-of-time-ordered correlators and the loschmidt echo in the quantum kicked top: how low can we go? Journal of Physics D: Applied Physics, 54(27):274004, 2021.

[27] Charles Neill, P Roushan, M Fang, Y Chen, M Kolodrubetz, Z Chen, A Megrant, R Barends, B Campbell, B Chiaro, et al. Ergodic dynamics and thermalization in an isolated quantum system. Nature Physics, 12(11):1037–1041, 2016.

[28] Zhixing Zou, Jiangbin Gong, and Weitao Chen. Enhancing quantum metrology by quantum resonance dynamics. Physical Review Letters, 134(23):230802, 2025.

[29] Ingemar Bengtsson and Karol Życzkowski. Geometry of quantum states: an introduction to quantum entanglement. Cambridge university press, 2017.

[30] Jonathan Kohler, Nicolas Spethmann, Sydney Schreppler, and Dan M Stamper-Kurn. Cavity-assisted measurement and coherent control of collective atomic spin oscillators. Physical Review Letters, 118(6):063604, 2017.

[31] Kevin C Cox, Graham P Greve, Joshua M Weiner, and James K Thompson. Deterministic squeezed states with collective measurements and feedback. Physical review letters, 116(9):093602, 2016.

[32] Justin G Bohnet, Brian C Sawyer, Joseph W Britton, Michael L Wall, Ana Maria Rey, Michael Foss-Feig, and John J Bollinger. Quantum spin dynamics and entanglement generation with hundreds of trapped ions. Science, 352(6291):1297–1301, 2016.

[33] Ian D Leroux, Monika H Schleier-Smith, and Vladan Vuletić. Implementation of cavity squeezing of a collective atomic spin. Physical Review Letters, 104(7):073602, 2010.

[34] Onur Hosten, Nils J Engelsen, Rajiv Krishnakumar, and Mark A Kasevich. Measurement noise 100 times lower than the quantum-projection limit using entangled atoms. Nature, 529(7587):505–508, 2016.

[35] A Kuzmich, L Mandel, J Janis, YE Young, R Ejnisman, and NP Bigelow. Quantum nondemolition measurements of collective atomic spin. Physical Review A, 60(3):2346, 1999.

[36] M Koschorreck, M Napolitano, B Dubost, and MW Mitchell. Quantum nondemolition measurement of large-spin ensembles by dynamical decoupling. Physical review letters, 105(9):093602, 2010.